Journal of Materials Chemistry C

RSC Publishing

PAPER

View Article Online
View Journal | View Issue

Water soluble pentacene†

Cite this: J. Mater. Chem. C, 2013, 1, 2193

Chandrani Pramanik,[a] Yushu Li,[a] Anup Singh,[b] Weimin Lin,[a] Jennifer L. Hodgson,[a] Jonathan B. Briggs,[a] Simka Ellis,[a] Peter Müller,[c] Nicol E. McGruer[b] and Glen P. Miller*[a]

Received 25th September 2012
Accepted 27th January 2013

DOI: 10.1039/c3tc00278k

www.rsc.org/MaterialsC

A water soluble pentacene, potassium 3,3′-(pentacene-6,13-diylbis(sulfanediyl))dipropanoate (**4**), has been synthesized and characterized. The synthesis of **4** is straightforward and scalable, and its isolation does not require time consuming chromatographic separations. UV-vis spectra in several solvents indicate an optical HOMO–LUMO gap of approximately 1.91–1.97 eV. Water soluble pentacene **4** is long-lived in the solution phase and in the solid state. Because it forms stable solutions, inks based on **4** have been formulated and printed onto paper and flexible plastic using an unmodified commercial ink-jet printer. A bi-layer photovoltaic cell using **4** as donor and [60]fullerene as acceptor was fabricated and shown to be active. The crystal structure of the pentacene diacid precursor to water soluble pentacene **4** has been solved and shows a parallel displaced arrangement of pentacene rings, indicative of stabilizing π–π stacking interactions. DFT modeling for **4**, however, suggests an unusual, low energy conformation in which both potassium carboxylate moieties are located on the same face (*syn*) of the pentacene π system. Likewise, calculated two-molecule stacks of **4** suggest a crystal packing arrangement in which potassium carboxylate moieties are intercalated between adjacent pentacene rings.

Introduction

Pentacene is considered a benchmark semiconductor in organic electronic devices due to its high charge carrier mobility ($\geq$1 $cm^2\ V^{-1}\ s^{-1}$).[1,2] Unfortunately, its solution processability is severely limited due to its poor solubility and its propensity to photodegrade within minutes in solutions exposed to light and air. The design and synthesis of functionalized pentacenes[3–10] with enhanced solubility and solution stability, face-to-face crystal packing arrangements and lower HOMO–LUMO gaps potentially allow for the fabrication of low cost, robust thin film devices[11–15] using solution based processing methods such as spin coating, blade coating, spray coating, ink-jet printing, *etc.* However, solution processed thin-film devices typically require a multi-layer construction in which successive layers are deposited from solvents of opposite polarity such that the deposition of each new film does not damage the preceding layer. Consequently, both hydrophobic (organic soluble) and hydrophilic (*e.g.*, water soluble) organic semiconductors are needed. Although pentacene and its functionalized derivatives are promising organic semiconductor compounds, no water soluble pentacene is known. Here, we describe the synthesis and characterization of the first water soluble pentacene.

Examples of thin-film electronic devices prepared from water soluble organic semiconductors include solar cells that utilize water soluble donors (*e.g.*, polythiophenes and phthalocyanines),[16–18] acceptors[19] or both[20–25] with power conversion efficiencies ranging from 0.17% to 0.39%. Several water soluble anthracene[26–29] and tetracene[30] derivatives are known, but they have not been utilized for thin film electronic applications and they are not expected to exhibit superior mobility as compared to a pentacene derivative.

Experimental section

General experimental details are provided in the ESI.†

syn-3,3′-((6,13-Dihydropentacene-6,13-diyl)bis(sulfanediyl)) dipropanoic acid (2)

A flame-dried, N_2 purged 250 mL round bottom flask was charged with ZnI_2 (4.08 g, 12.78 mmol), 6,13-dihydro-6,13-dihydroxypentacene (**1**) (2.00 g, 6.40 mmol) and 190 mL dry CH_2Cl_2. To this mixture was added 3-thiopropanoic acid (1.3 mL, 14.91 mmol) and the resulting pink reaction mixture was stirred for 24 hours. A white solid precipitated over the course of the reaction and was isolated by filtration and thoroughly washed with CH_2Cl_2 followed by warm water. Upon drying *in vacuo* for 24 hours, compound **2** was isolated as an off-white solid (3.03 g, 97%). An X-ray quality single crystal of **2** was grown by slow evaporation of a saturated solution in acetone. ^1H

[a]Department of Chemistry & Materials Science Program, University of New Hampshire, Durham, NH 03824, USA. E-mail: glen.miller@unh.edu

[b]Department of Electrical and Computer Engineering, Northeastern University, Boston, MA 02115, USA

[c]Department of Chemistry, Massachusetts Institute of Technology, Cambridge, MA 02139, USA

† Electronic supplementary information (ESI) available. CCDC 902874 (**3**) and 902875 (**2**). For ESI and crystallographic data in CIF or other electronic format see DOI: 10.1039/c3tc00278k

NMR (400 MHz, CD_3OD) δ (ppm): 7.95 (s, 4H), 7.93–7.86 (m, 4H), 7.53–7.46 (m, 4H), 5.59 (s, 2H), 2.97 (t, 4H, $J = 7.3$ Hz), 2.68 (t, 4H, $J = 7.3$ Hz); ^{1}H NMR (400 MHz, DMSO-d_6) δ (ppm): 12.32 (bs, 2H), 8.03 (s, 4H), 7.98–7.90 (m, 4H), 7.57–7.49 (m, 4H), 5.67 (s, 2H), 2.91 (t, 4H, $J = 7.2$ Hz), 2.67 (t, 4H, $J = 7.2$ Hz); ^{13}C NMR (100 MHz, DMSO-d_6) δ (ppm): 173.17, 135.37, 132.04, 127.52, 127.18, 126.39, 46.74, 34.34, 28.29; ^{13}C NMR (125 MHz, CD_3OD): δ (ppm): 176.02, 136.38, 134.01, 128.66, 128.61, 127.36, 35.52, 29.38. LDI-MS m/z: 490.4 [M + 2]; ESI HRMS: [M^+ + Na] 511.1032 (calculated 511.1008, error −4.7 ppm); IR (COOH 1705 cm^{-1}). Melting point: the white solid started to slowly melt and change color in an open capillary tube at 135 °C and was completely melted at 140 °C as a blue-purple liquid.

3,3′-(Pentacene-6,13-diylbis(sulfanediyl))dipropanoic acid (3)

A flame dried, Ar purged 150 mL pressure vessel was charged with **2** (1.50 g, 3.07 mmol), chloranil (1.134 g, 4.61 mmol) and benzene (120 mL). The vessel was sealed with a Teflon screw cap. The mixture was heated with stirring to 100 °C in an oil bath for 24 hours in the dark. After cooling to room temperature, the reaction mixture was filtered and washed successively with benzene, hexanes and hot water (60 °C). After drying *in vacuo* overnight, pentacene **3** was isolated as a dark blue solid (1.05 g, 2.16 mmol, 70%). An X-ray quality crystal of **3** was grown from a supersaturated solution of acetic acid. ^{1}H NMR (500 MHz, CD_3COOD) δ (ppm): 9.81 (s, 4H), 8.21–8.13 (m, 4H), 7.53–7.46 (m, 4H), 3.41 (t, 4H, $J = 6.9$ Hz), 2.64 (t, 4H, $J = 6.9$ Hz); ^{1}H NMR (500 MHz, CD_3OD) δ (ppm): 9.75 (s, 4H), 8.13–8.07 (m, 4H), 7.48–7.42 (m, 4H), 2.47 (t, 4H, $J = 6.8$ Hz); ^{1}H NMR (500 MHz, acetone-d_6) δ (ppm): 9.82 (s, 4H), 8.22–8.15 (m, 4H), 7.53–7.46 (m, 4H), 3.36 (t, 4H, $J = 7.0$ Hz), 2.54 (t, 4H, $J = 7.0$ Hz). ^{13}C NMR (125 MHz, CD_3COOD, 80 °C) δ (ppm): 134.24, 133.78, 129.89, 127.94, 127.31, 35.60, 33.35 (coincidental overlap of one aromatic signal; low intensity C=O signal is not observed). LDI-MS m/z: 486.1 [M^+]; ESI HRMS: [M^+] 487.1053 (calculated 487.1032, error −4.3 ppm); IR (COOH: 1698 cm^{-1}); UV-vis: 527, 570 and 612 nm in CH_3OH; 534, 575 and 623 nm in $CHCl_3$; 529, 566 and 614 nm in $(CH_3)_3CO$. Melting point: 235 °C.

Potassium 3,3′-(pentacene-6,13-diylbis(sulfanediyl)) dipropanoate (4)

A flame dried, Ar purged 250 mL round bottom flask was charged with **3** (0.80 g, 1.64 mmol), K_2CO_3 (0.908 g, 6.57 mmol), and absolute ethanol (250 mL). The reaction mixture was stirred in the dark at room temperature for 3 hours under Ar. After removing excess K_2CO_3 by filtration, the filtrate was concentrated under reduced pressure. The crude blue solid was thoroughly washed with chloroform, acetone and hexane and recovered in 84% yield. Crude water soluble pentacene **4** was then re-dissolved in ethanol (200 mL) and diluted with hexane (200 mL). Upon cooling overnight at 10 °C, pure **4** was isolated by filtration as a shiny blue polycrystalline solid (0.711 g, 77% isolated yield from **3**). ^{1}H NMR (400 MHz, D_2O) δ (ppm): 8.81 (s, 4H), 7.72–7.57 (m, 4H), 7.31–7.15 (m, 4H), 2.84 (t, 4H, $J = 7.2$ Hz), 2.02 (t, 4H, $J = 7.2$ Hz); ^{1}H NMR (500 MHz, CD_3OD) δ (ppm): 9.69 (s, 4H), 8.07–8.02 (m, 4H), 7.42–7.36 (m, 4H), 3.27–3.22 (pseudo-t, 4H), 2.42–2.37 (pseudo-t, 4H); ^{13}C NMR (125 MHz, D_2O) δ (ppm): 174.97, 125.50, 125.31, 124.51, 122.69, 120.33, 120.05, 31.73, 28.06; ^{13}C NMR (125 MHz, D_2O with K_2CO_3 as internal reference) δ (ppm): 174.97, 160.64 (K_2CO_3), 125.56, 125.40, 124.63, 122.72, 120.38, 120.12, 31.73, 28.08; ^{13}C NMR (125 MHz, CD_3OD) δ (ppm): 180.03, 133.92, 133.54, 133.49, 129.72, 127.83, 127.00, 39.64, 35.54. MALDI-MS (S_8 matrix) m/z: 562.9 [M^+]; ESI HRMS: [M^+] 563.018 (calculated 563.0150, error −5.8 ppm); IR (COOK: 1560 and 1390 cm^{-1}); UV-vis: (538, 575 and 621 nm in pH 10 buffer; 532, 573 and 619 nm in H_2O; 526, 565 and 611 nm in CH_3OH). Melting point: 276 °C (**4** does not melt between 25 °C and 500 °C when the solid is heated slowly. There is a subtle color change from blue to purple during this slow heating. However, freshly prepared samples in open capillary tubes melt sharply at 276 °C or higher when heated quickly *via* immersion of room temperature capillary tubes into the melting point apparatus at temperature).

Bilayer solar cell

Bi-layer solar cells with the configuration ITO/PEDOT:PSS/**4**/C_{60}/Al were fabricated. Indium tin oxide (ITO) coated glass (ITO: 140 nm, glass: 1.1 mm, sheet resistance: 20 Ω $\square^{-1}$, Delta Technologies) was diced into 15 × 15 mm chips that were cleaned by ultrasonication in soap water, followed by a DI water rinse, followed by successive ultrasonications (10 min each) in acetone and isopropyl alcohol. Following this, the chips were again rinsed with DI water. After oven drying for 1 hour at 150 °C, the chips were cleaned using an ICP oxygen plasma treatment (300/50 W, plasma/bias power in a Plasma-Therm 7900 etcher) rendering the ITO surface hydrophilic. A solution of PEDOT:PSS (high-conductivity grade from Sigma-Aldrich) was filtered through a 0.45 μm syringe filter and spin coated onto clean substrates at 4000 rpm. The chips were then baked for 20 min at 120 °C, yielding an 80 nm PEDOT:PSS film. Spin coating and thermal annealing of water soluble pentacene **4** were performed inside a glove box (oxygen < 1 ppm, H_2O < 1 ppm) under nitrogen. A solution of **4** (1 wt%) in ethanol was prepared and filtered through a 0.45 μm syringe filter. An infrared lamp (250 W) was used to heat both the substrate and the solution of **4** to 60–80 °C just prior to spin coating. The hot solution of **4** was spin coated onto hot substrate at 2000 rpm for 1 minute followed by thermal annealing at 120 °C for 2 minutes on a hot plate. Outside of the glove box, a 25 nm film of C_{60} (99.95% from SES Research) and a 110 nm film of aluminum were then deposited in successive steps, the latter through a shadow mask, *via* thermal evaporation with a base pressure of 5×10^{-7} Torr. Top view images of PEDOT:PSS/**4**/C_{60} were taken using an optical microscope (Accu-Tech Optical Inc) connected to a 3 MP digital camera. The thickness of the films was measured using a Dektak3ST Profilometer. *J–V* data was acquired with a 4155A HP Semiconductor Parameter Analyzer. The photocurrent was measured under the illumination of a halogen lamp (Dolan Jenner Fiber-lite), which was calibrated to generate 0.4 times the short circuit current (J_{SC}) of natural sunlight with an intensity of 63 mW cm^{-2}.

Results and discussion

Synthesis of pentacene diacid 3 and water soluble pentacene 4

The synthesis of pentacene diacid **3** and water soluble pentacene **4** proceeded as illustrated in Fig. 1. Compound 6,13-dihydro-6,13-dihydroxypentacene (**1**) was synthesized following a reported procedure.[31] Thiol coupling to afford *syn*-3,3′-((6,13-dihydropentacene-6,13-diyl)bis(sulfanediyl))dipropanoic acid (**2**) was achieved *via* a modified Kobayashi procedure.[9] After filtering and solvent washing, a single diastereomer of **2** was isolated in 97% yield as a white solid. An X-ray quality crystal was grown from a saturated solution in acetone. The X-ray structure (see ESI†) was subsequently solved, revealing *syn* stereochemistry for **2**.

The chloranil oxidation of **2** to produce 3,3′-(pentacene-6,13-diylbis(sulfanediyl))dipropanoic acid (**3**) worked best when 1.5 equivalents of chloranil were utilized in a sealed reaction vessel in the absence of potassium carbonate. The reaction was attempted using either toluene as solvent at 130 °C or benzene as solvent at 100 °C. In both cases, blue solids precipitated and were filtered followed by thorough washing with benzene, hexane and hot water. For reactions run in toluene at 130 °C, the blue solids formed within 3 hours and corresponded to insoluble anhydride oligomers, not pentacene diacid **3**. The anhydride was efficiently converted to potassium 3,3′-(pentacene-6,13-diylbis(sulfanediyl)) dipropanoate **4** using a saturated solution of potassium carbonate in ethanol. However, the yield of isolated anhydride was found to vary with scale. Thus, when utilizing 50 mg of **2**, the chloranil oxidation in toluene at 130 °C produced anhydride oligomers in 48% yield. Upon moving to 100 mg, 500 mg and 700 mg scales, the corresponding yields dropped to 24%, 20% and 14%, respectively. For chloranil oxidation reactions run in benzene at 100 °C, the isolated blue product is pentacene diacid **3**, not anhydride. The reactions run in benzene at 100 °C were slower (typically 24 h reaction time) but they produced higher yields of product and were scalable. For example, when the chloranil oxidation was run in benzene at 100 °C using 1.5 grams of **2**, 1.05 grams of pentacene diacid **3** was isolated corresponding to a 70% yield.

Treatment of diacid **3** with potassium carbonate in ethanol followed by filtration, evaporation and simple solvent washing yielded amorphous, blue, water soluble pentacene **4** in 84% crude yield. To remove any residual potassium carbonate, the pentacene salt was redissolved in ethanol, filtered, and the solution was diluted with hexane. Upon cooling to 10 °C, pure polycrystalline **4** was recovered by filtration in 77% isolated yield from diacid **3**.

Pentacene diacid **3** shows limited to decent solubility in a variety of solvents including methanol, acetone, acetic acid, THF, DMSO and DMF. The solutions are stable for a minimum of a few days, excepting the case of THF where degradation to give a yellow solution is observed within 24 hours. Diacid **3** precipitates somewhat rapidly from methanol, ethanol, acetone and acetic acid, suggesting rapid aggregation in those solutions. Likewise, an X-ray quality crystal of diacid **3** was prepared from a supersaturated solution in acetic acid. A parallel displaced arrangement of pentacene backbones is observed in the extended structure (Fig. 2), a geometry suitable for charge hopping (charge carrier mobility) throughout the crystal, as required in associated thin film electronic devices.[32] The shortest π–π distance between neighboring pentacene rings is 3.52 Å. The single crystal prepared from acetic acid includes two acetic acid molecules for every molecule of diacid **3**.

Compound **4** is soluble in a variety of polar solvents including water, methanol, ethanol, DMSO and DMF. In aqueous solution, **4** and diacid **3** can be interconverted (Scheme 1). For example, a suspension of solid diacid **3** in water is converted to a solution of **4** upon addition of base. Likewise, solid **3** precipitates from an aqueous solution of **4** upon addition of acid.

Spectroscopic and physical characterization of pentacene diacid 3 and water soluble pentacene 4

Pentacene diacid **3** and water soluble pentacene **4** have been extensively characterized using ^{1}H and ^{13}C NMR spectroscopies,

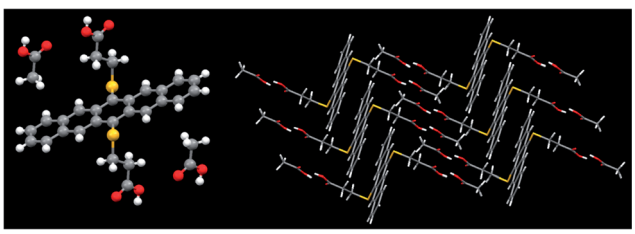

Fig. 2 X-ray crystal structure of pentacene diacid **3** that is deprotonated in basic solution to form water soluble pentacene **4**. The single crystal was prepared from a saturated solution in acetic acid. Left: pentacene diacid **3** plus two acetic acid molecules in the crystal structure. Right: parallel displaced stacking arrangement of pentacene backbones in the crystal structure of **3**.

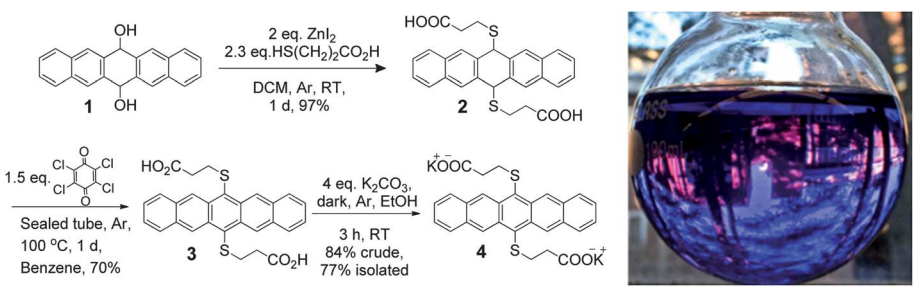

Fig. 1 Left: synthesis of water soluble pentacene **4**; right: a solution of **4** in water.

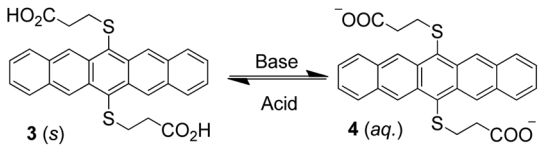

Scheme 1 Interconversion of pentacene diacid **3** (s) and water soluble pentacene **4** (aq.).

electrospray ionization high resolution mass spectrometry, MALDI mass spectrometry, IR spectroscopy, UV-vis spectroscopy, melting point and thermogravimetric analysis (TGA).

The ^{1}H NMR spectrum of **4** recorded in D_2O includes a singlet at 8.81 ppm corresponding to the four aromatic (*X*) protons at the 5, 7, 12 and 14 positions of the pentacene backbone. Multiplets at 7.72–7.57 and 7.31–7.15 ppm correspond to the remaining aromatic (AA′MM′) protons, consistent with other 6,13-disubstituted pentacenes. A pair of triplets at 2.84 and 2.02 ppm is also observed corresponding to the two separate sets of methylene protons on the 6,13-diorganothio substituents. The ^{13}C NMR spectrum consists of 2 alkyl signals (37.2 and 33.5 ppm), 6 aromatic signals (130.9–125.5 ppm) and 1 carbonyl signal (175 ppm), as expected. The IR spectrum of diacid **3** shows a carboxylic acid stretching vibration at 1698 cm^{-1}, whereas salt **4** shows two stretching vibrations at 1560 cm^{-1} and 1390 cm^{-1} (Fig. 3), similar to those observed for potassium acetate.

In the solid state, **4** is indefinitely stable when refrigerated and protected from light. Crystalline **4** does not melt when heated slowly in an open capillary tube from room temperature to 500 °C. However, **4** melts sharply without decomposition at 276 °C or higher when heated quickly from room temperature to melting temperature in a pre-heated melting point apparatus. A thermogravimetric analysis (TGA) plot for **4** (ramp rate 5 °C min^{-1}) reveals ~9% weight loss between room temperature and 200 °C in both air and N_2. This loss is likely associated with the evaporation of occluded solvent. Further ~30% and ~50% weight losses are observed between ~240 and 500 °C for samples heated in N_2 and air, respectively, with most of the losses occurring between 300 and 500 °C, well beyond the recorded melting point for **4**. Crystalline diacid **3** melts sharply at 235 °C in a melting point apparatus without decomposition, even with slow heating. However, TGA plots for **3** in air and N_2 reveal ~14 to 18% weight loss events between 235 and 300 °C, likely associated with escape of occluded solvent. The crystal structure for **3** includes two acetic acid molecules for every diacid (~20% acetic acid by weight). We conclude that both pentacene diacid **3** and water soluble pentacene **4** are relatively robust species with a high degree of thermal stability and oxidative resistance.

UV-vis spectra for water soluble pentacene **4** in methanol, water and aqueous buffer are shown in Fig. 4. The λ_{max} values for the longest wavelength absorptions vary slightly with solvent (water: 619 nm; pH 10 buffer: 621 nm; methanol: 611 nm). From the onset of absorptions, an optical HOMO–LUMO gap for **4** of 1.91–1.97 eV is indicated. For comparison, the optical band gap for pentacene in *o*-dichlorobenzene is 2.08 eV.[10] HOMO and LUMO energies for **4** of −5.16 and −3.43 eV, respectively, were calculated at the TD-B3LYP/6-311+G(d,p)//B3LYP/6-31G(d) level of theory in an aqueous medium (implementing the PCM solvation method) in order to match other calculations reported (see below). The calculated HOMO–LUMO gap for **4** of 1.73 eV is about 0.2 eV smaller than the measured optical gap.

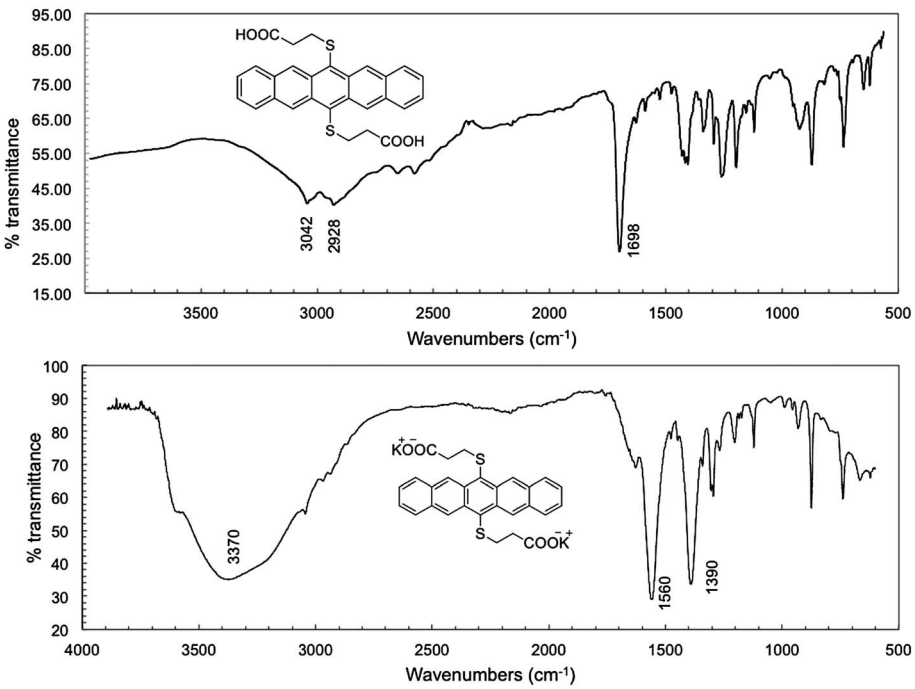

Fig. 3 IR spectra of pentacene diacid **3** (top) and water soluble pentacene **4** (bottom).

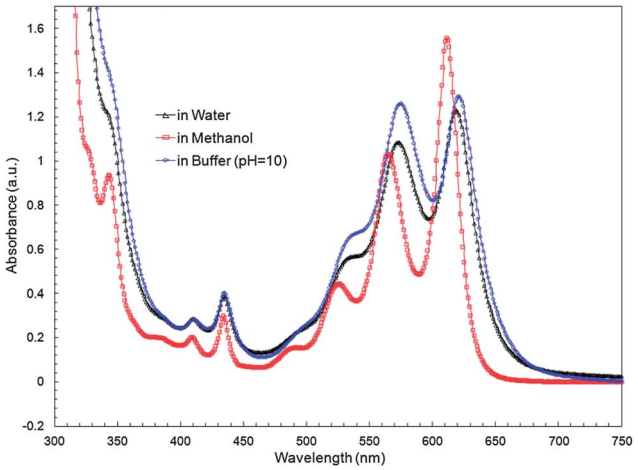

Fig. 4 UV-vis spectra of **4** in water, buffer solution (pH 10) and methanol.

The longest λ_{max} values for diacid **3** also vary slightly with solvent (methanol: 612 nm; $CHCl_3$: 623 nm; acetone: 614 nm) but are overall quite similar to those of **4**. From the onset of absorptions, an optical HOMO–LUMO gap of 1.93–1.96 eV is indicated for **3**. The half-life of **4** in aqueous buffer solution with exposure to light and air is approximately four days (5786 min), making it one of the most solution-stable pentacene derivatives known.[10]

Modeling of water soluble pentacene 4

The structure and energetics of **4** were examined using density functional theory methods. The large conformational space of **4** in the gas phase and in aqueous medium was first explored. Table 1 shows the structures of several of the most important conformers and gives an overview of the space. The relative energies of the conformers are shown at the B3LYP/6-311+G(d,p)//B3LYP/6-31G(d) level when optimized in the gas phase, and in an aqueous medium represented using the polarizable continuum model (PCM)[33] as implemented in the Gaussian 03 software package.[34] Many other local minima exist, all with relative energies within the range shown in Table 1.

From Table 1, it is evident that the lowest energy conformations in the gas phase place the positively charged potassium atoms of the CO_2K groups above one of the pentacene rings, indicative of a stabilizing cation–π interaction. A comparison of conformers B and D suggests that each cation–π interaction in conformer B lowers its energy by approximately 4 kcal mol^{-1}. Cation–π interactions between alkali metal cations and benzene rings are well known. Two recent theoretical studies using B3LYP and MP2 methods calculated distances of 2.86 Å and 2.90 Å, respectively, between K^+ and the center of a single benzene molecule, and 2.96 Å and 2.93 Å when the K^+ is sandwiched between the centers of two parallel benzene molecules.[35,36] In crystal form, these types of sandwich structures are influenced by the presence of counter ions and have been measured in two previous cases as having slightly longer distances of 3.14 Å for a $[K(C_6H_5)_2]^+[CB_{11}Me_{12}]^-$ system[37] and 2.986 Å for a $K[B(C_6H_5)_4]$ system.[38] The low energy conformers of

Table 1 Relative energies in the gas phase (E_{gas}) and in aqueous solution (E_{solvn}) of symmetric conformers of water soluble pentacene **4**[a]

Conformer	Structure	E_{gas} (kcal mol^{-1})	E_{solvn} (kcal mol^{-1})
A	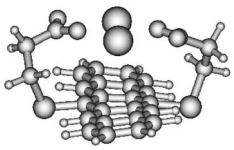	0	0
B	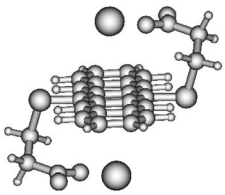	24.4	11.3
C	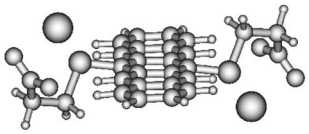	31.4	8.2
D	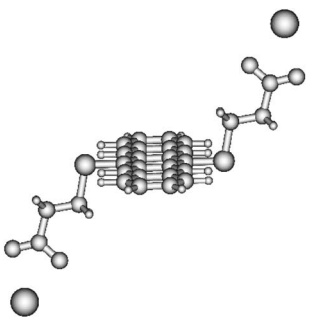	31.9	4.7
E	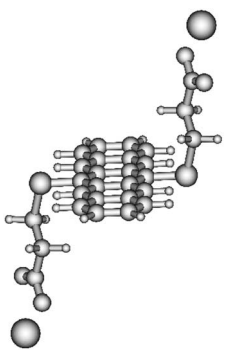	32.2	5.3
F	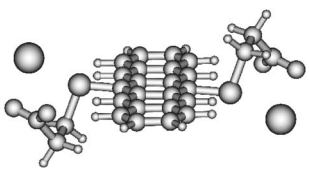	32.9	10.5

[a] At the B3LYP/6-311+G(d,p)//B3LYP/6-31G(d) level. Optimizations and single-point energies in an aqueous medium were represented using the polarizable continuum model (PCM) with the recommended radii for these calculations (*i.e.*, the united atom topological model applied to radii optimized for the PBE0/6-31G(d) levels of theory).

4 in Table 1 show cation–π interactions that have slightly longer distances from K^+ to the center of the associated benzene rings, 3.26 Å and 3.08 Å for conformers A and B, respectively. In the lowest energy conformer A, the K^+ cations are offset from the centers of penultimate rings in order to simultaneously coordinate to three separate oxygen atoms as well as the π-system of the pentacene (Fig. 5). This complex binding with both K^+ cations located on the same face of conformer A (*i.e.*, *syn* arrangement) is energetically preferred by almost 25 kcal mol^{-1} compared to conformer B where the K^+ cations are located on opposite faces (*i.e.*, *anti* arrangement). Fig. 5 shows the arrangement of charges in the CO_2K groups and the distances between the atoms for conformer A.

In the presence of a solvent field, the relative energies of conformers A–F fall within a smaller range of values due to stabilization imparted by the field onto the molecules. This solvation stabilization is greatest when ethylthio substituents are extended from the molecule, as in conformers D and E, allowing for more interaction between the polar CO_2K groups and the aqueous medium. While conformers D and E are favorable in an aqueous medium, the complex binding shown in conformer A with *syn* arrangement of K^+ cations remains the lowest energy conformer.

Table 1 shows discrete water soluble pentacene **4** conformers optimized in the gas phase and in a solvent medium, but it does not necessarily indicate the arrangement of **4** in its crystal form. Fig. 6 shows the optimized geometries of two possible two-molecule stacks of **4**. Fig. 6a illustrates the stacking arrangement of two molecules of conformer B and includes four cation–π interactions, two located on the interior of the stack (akin to conformer A of Table 1) and two located on exterior faces of the stack (akin to conformer B of Table 1). Fig. 6b illustrates the stacking of two molecules of conformer E and also mimics the crystal packing seen in the X-ray crystal structure of the corresponding pentacene diacid **3** (Fig. 2) in which the primary interaction is π–π stacking between parallel displaced pentacenes. At the B3LYP/6-311+G(d,p)//B3LYP/6-31G(d) level, the relative energy of the structure shown in Fig. 6b is 18.0 kcal mol^{-1} higher than that of the structure shown in Fig. 6a. Apparently, stabilization of ions is energetically more important than π–π stacking in solid state **4**. We tentatively predict the crystal structure of **4** to resemble the two molecule stack of Fig. 6a. Thus far, all attempts to prepare X-ray quality single crystals of **4** have failed. As its solid state structure critically impacts its thin-film device properties, we continue to investigate structural details of crystalline and thin-film water soluble pentacene **4**.

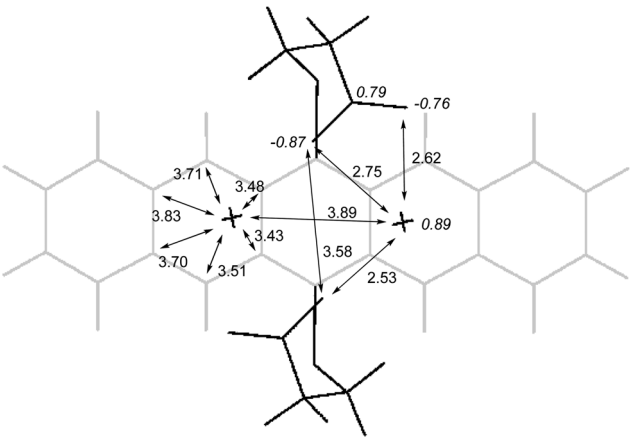

Fig. 5 The C_2 symmetric structure of the lowest energy conformation of water soluble pentacene **4** (conformer A) showing distances (Å) between atoms in the CO_2K groups, and between K^+ (*X*) and the carbons in the penultimate ring of pentacene. NBO charges on atoms in the CO_2K groups (at the B3LYP/6-311+G(d,p)//B3LYP/6-31G(d) level) are shown in italics.

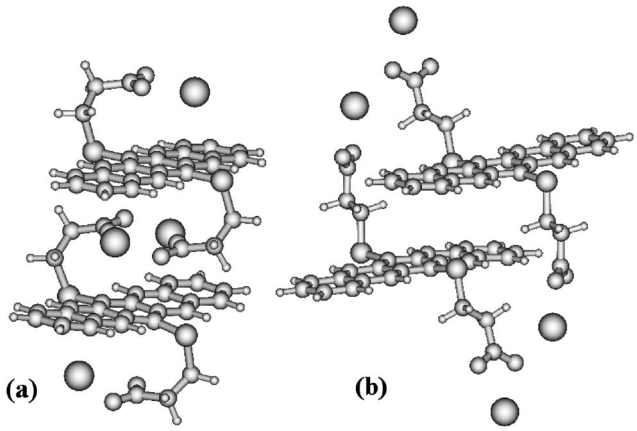

Fig. 6 B3LYP/6-31G(d) optimized geometries of two possible two-molecule stacks of water soluble pentacene based on conformer B (a) and conformer E (b) of Table 1.

Ink-jet printing of water soluble pentacene 4

Several inks suitable for ink-jet printing were formulated. Thus, a mixed solvent aqueous ink solution (10 mg mL^{-1} **4** in water, glycerol and ethylene glycol [85 : 9 : 6 by weight]), a DMSO based ink (8 mg mL^{-1} **4**) and an alcoholic ink (6.6 mg mL^{-1} **4** in 2 : 1 ethanol : methanol) were all prepared and successfully printed using an unmodified commercial ink-jet printer (Epson C88+). Prior to printing, the inks were purged with Ar and filtered through a 0.45 μm PTFE membrane filter. Refillable

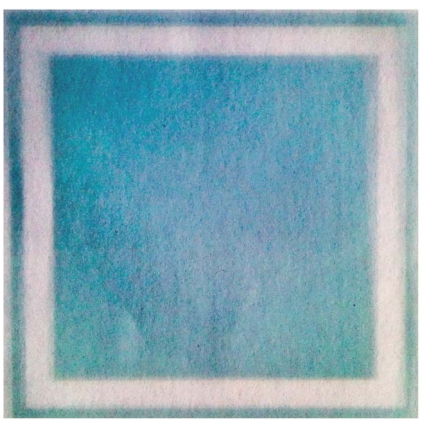

Fig. 7 Image of water soluble pentacene **4** ink-jet printed onto a flexible plastic substrate (Novele polyimide photopaper) using a DMSO based ink.

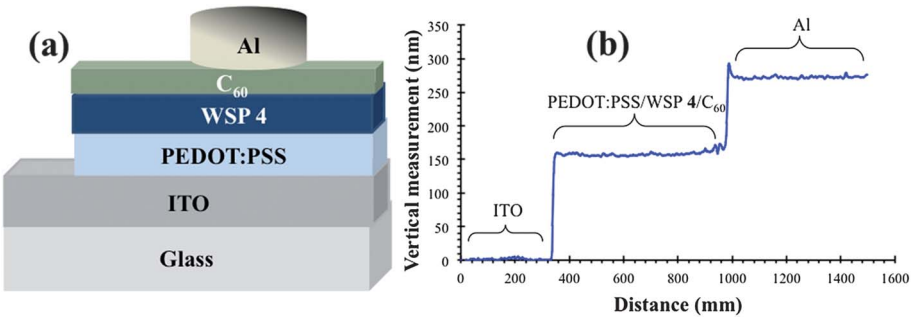

Fig. 8 Schematic of a bilayer organic solar cell fabricated using water soluble pentacene **4** (a) and composite Dektak profilometer scan (b).

ink-jet cartridges were also purged with Ar before filling with each ink solution. The inks were printed onto standard printer paper as well as a flexible plastic substrate (Novele polyimide photopaper, Novacentrix) as illustrated in Fig. 7. The printed samples were thermally annealed between 120 and 130 °C for 1–5 minutes.

Preliminary bilayer photovoltaic devices

A schematic for a bilayer solar cell with the configuration ITO/PEDOT:PSS (80 nm)/**4** (55 nm)/C_{60} (25 nm)/Al (110 nm) is shown in Fig. 8a along with the corresponding Dektak profilometer scan in Fig. 8b.

Initially, we attempted to prepare a thin-film of water soluble pentacene **4** *via* spin coating onto PEDOT:PSS at room temperature using DI water as solvent. However, the PEDOT:PSS layer was visibly damaged in the presence of the slightly basic aqueous solution (pH ~ 7.5 for a 1 mg mL^{-1} solution). Upon spin coating an alcoholic solution of **4** at room temperature, the PEDOT:PSS layer remained intact but micro crystals of water soluble pentacene were observed to form as illustrated in Fig. 9a. Uniform films of **4** were ultimately formed (Fig. 9b) by spin coating a hot ethanolic solution (60–80 °C) onto hot substrate such that the rate of evaporation of ethanol exceeded the rate of crystal formation.

Despite a lack of optimization, the water soluble pentacene–C_{60} bilayer devices all showed a significant photovoltaic response (Table 2). Open-circuit voltages (V_{OC}) and short circuit current densities (J_{SC}) were measured while the fill factors (FF) and power conversion efficiencies (PCE) were calculated after correcting for the incandescent light source. A consistent V_{OC} of approximately 0.5 V was observed in all cells. The best cell (Sample 1, Table 2) had a FF of 0.32 and a V_{OC} of 0.53 V. The measured J_{SC} for this cell (0.125 mA cm^{-2}) was low, leading to a corrected PCE of 0.084%.

Table 2 Performance of unoptimized bilayer solar cells (ITO/PEDOT:PSS (80 nm)/**4** (55 nm)/C_{60} (25 nm)/Al (110 nm)) using water soluble pentacene **4** as donor and C_{60} as acceptor

Sample	J_{SC} (mA cm^{-2})	V_{OC} (V)	FF	PCE[a] (%)
1	0.125	0.53	0.322	0.084
3	0.116	0.58	0.209	0.056
4	0.102	0.50	0.228	0.048
5	0.112	0.52	0.243	0.056

[a] Tested under a halogen light calibrated to generate 0.4 times the short-circuit current with sunlight of 63 mW cm^{-2}. Hence, the best PCE is $0.021/(0.4 \times 0.63) = 0.084\%$.

We observed a pronounced S-shaped *J–V* curve[39–41] near the open-circuit condition for bilayer solar cells as illustrated in Fig. 10, leading to reduced fill factors. The S-shaped dependence could be a contact-driven process[41] due to formation of barriers for carrier extraction[39] created by interfacial dipoles, defects, traps or charge carrier accumulation. Optimization of the photovoltaic cells is planned, including optimization of the

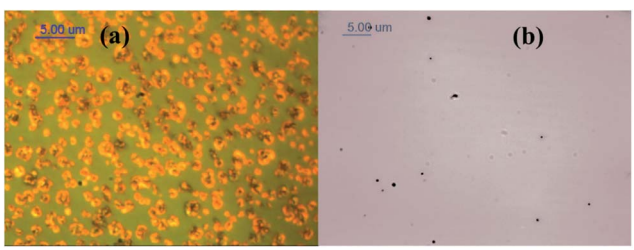

Fig. 9 Optical images of thin films of C_{60} atop water soluble pentacene **4** and PEDOT:PSS (C_{60}/**4**/PEDOT:PSS) when (a) the water soluble pentacene layer was spin coated at room temperature and (b) the water soluble pentacene layer was spin coated at 60–80 °C. Microcrystalline **4** and a lack of thin-film continuity is observed in (a) while (b) illustrates a largely continuous thin-film with occasional defects.

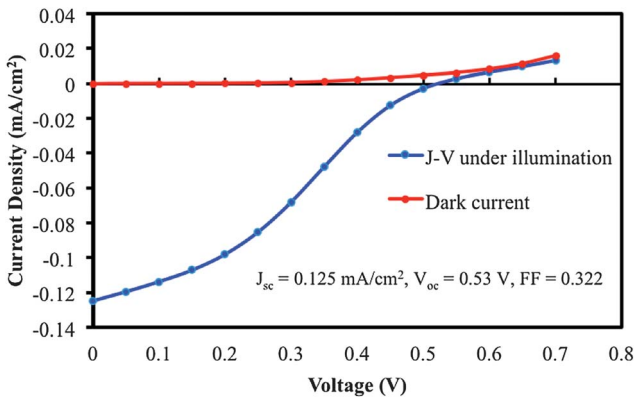

Fig. 10 *J–V* curves for sample 1 of Table 2 in the dark and under illumination conditions (calibrated halogen lamp).

active layer thicknesses in order to increase short circuit current densities.

Conclusions and future direction

We successfully synthesized and isolated a water soluble pentacene, potassium 3,3′-(pentacene-6,13-diylbis(sulfanediyl)) dipropanoate (**4**). Water soluble pentacene **4** was synthesized in three steps from pentacene-6,13-diol, the last involving deprotonation of the corresponding pentacene diacid **3**. The synthesis of **4** is straightforward and scalable, and its isolation does not require time consuming chromatographic separations. Water soluble pentacene **4** has been extensively characterized using NMR, IR and UV-vis spectroscopies as well as laser desorption ionization and high resolution mass spectrometries, melting point determination and thermal gravimetric analysis. It is a robust pentacene derivative with excellent solution phase and solid-state stabilities. UV-vis spectra in several solvents indicate an optical HOMO–LUMO gap of approximately 1.91–1.97 eV. A photodegradation study indicates that aqueous solutions of **4** are stable for days. Several water soluble pentacene inks were formulated and successfully printed onto paper and flexible plastic using an unmodified commercial ink-jet printer. Unoptimized bilayer photovoltaic cells using **4** as donor and C_{60} as acceptor were constructed and shown to be active. The crystal structure of the pentacene diacid precursor to **4**, compound **3**, has been solved and shows a parallel displaced arrangement of pentacene rings, indicative of stabilizing π–π stacking interactions. DFT modeling indicates an unusual conformation for water soluble pentacene **4** in both the gas phase and in polar media, one in which both potassium carboxylate moieties are located on the same face (*syn*) of the pentacene π-system. Likewise, calculated two-molecule stacks of **4** suggest a crystal packing arrangement in which potassium cations are intercalated between adjacent pentacene rings.

Future work will include continued structural investigations of crystalline and thin-film **4** as well as optimization of photovoltaic cells and the fabrication of other thin-film electronic devices prepared from **4**.

Acknowledgements

This work was funded by the National Science Foundation through the Nanoscale Science & Engineering Center for High-rate Nanomanufacturing (grant NSF EEC-0832785). The authors also acknowledge Professor Edward Wong for helpful discussions and Amit Tripathi for technical assistance.

References

1 H. Klauk, M. Halik, U. Zschieschang, G. Schmid and W. Radlik, *J. Appl. Phys.*, 2002, **92**, 5259.
2 S. Lee, B. Koo, J. Shin, E. Lee, H. Park and H. Kim, *Appl. Phys. Lett.*, 2006, **88**, 162109.
3 Q. Miao, X. Chi, S. Xiao, R. Zeis, M. Lefenfeld, T. Siegrist, M. L. Steigerwald and C. Nuckolls, *J. Am. Chem. Soc.*, 2006, **128**, 1340.
4 J. Chen, S. Subramanian, S. R. Parkin, M. Siegler, K. Gallup, C. Haughn, D. C. Martin and J. E. Anthony, *J. Mater. Chem.*, 2008, **18**, 1961.
5 S. Katsuta, D. Miyagi, H. Yamada, T. Okujima, S. Mori, K. Nakayama and H. Uno, *Org. Lett.*, 2011, **13**, 1454.
6 J. E. Anthony, J. S. Brooks, D. L. Eaton and S. R. Parkin, *J. Am. Chem. Soc.*, 2001, **123**, 9482.
7 Y. Sakamoto, T. Suzuki, M. Kobayashi, Y. Gao, Y. Fukai, Y. Inoue, F. Sato and S. Tokito, *J. Am. Chem. Soc.*, 2004, **126**, 8138.
8 E. Clar and B. Dtsch, *Ber. Dtsch. Chem. Ges. B*, 1932, **65**, 503.
9 K. Kobayashi, R. Shimaoka, M. Kawahata, M. Yamanaka and K. Yamaguchi, *Org. Lett.*, 2006, **8**, 2385.
10 I. Kaur, W. Jia, R. P. Kopreski, S. Selvarasah, M. R. Dokmeci, C. Pramanik, N. E. McGruer and G. P. Miller, *J. Am. Chem. Soc.*, 2008, **130**, 16274.
11 S. K. Park, T. N. Jackson, J. E. Anthony and D. A. Mourey, *Appl. Phys. Lett.*, 2007, **91**, 063514.
12 A. A. Gorodetsky, M. Cox, N. J. Tremblay, I. Kymissis and C. Nuckolls, *Chem. Mater.*, 2009, **21**, 4090.
13 L. C. Palilis, P. A. Lane, G. P. Kushto, B. Purushothaman, J. E. Anthony and Z. H. Kafafi, *Org. Electron.*, 2008, **9**, 747.
14 Y. Jiang, S. Hong, J. H. Oh, R. Mondal, T. Okamoto, E. Verploegen, M. F. Toney, M. D. McGeheec and Z. Bao, *J. Mater. Chem.*, 2012, **22**, 4356.
15 M. T. Lloyd, A. C. Mayer, A. S. Tayi, A. M. Bowen, T. G. Kasen, D. J. Herman, D. A. Mourey, J. E. Anthony and G. G. Malliaras, *Org. Electron.*, 2006, **7**, 243.
16 J. Yang, A. Garcia and T.-Q. Nguyen, *Appl. Phys. Lett.*, 2007, **90**, 103514.
17 H. Benten, N. Kudo, H. Ohkita and S. Ito, *Thin Solid Films*, 2009, **517**, 2016.
18 S. Schumann, R. A. Hatton and T. S. Jones, *J. Phys. Chem. C*, 2011, **115**, 4916.
19 J.-F. Nierengarten, *New J. Chem.*, 2004, **28**, 1177.
20 Q. Qiao and J. T. McLeskey Jr, *Appl. Phys. Lett.*, 2005, **86**, 153501.
21 J. T. McLeskey Jr and Q. Qiao, *Int. J. Photoenergy*, 2006, 20951.
22 Q. Qiao, Y. Xie and J. T. McLeskey, *J. Phys. Chem. C*, 2008, **112**, 9912.
23 Q. Qiao, L. Su, J. Beck and J. T. McLeskey, *J. Appl. Phys.*, 2005, **98**, 094906.
24 J. K. Mwaura, M. R. Pinto, D. Witker, N. Ananthakrishnan, K. S. Schanze and J. R. Reynolds, *Langmuir*, 2005, **21**, 10119.
25 Z. Liu, L. Liu, H. Li, Q. Dong, S. Yao, A. B. Kidd IV, X. Zhang, J. Li and W. Tian, *Sol. Energy Mater. Sol. Cells*, 2012, **97**, 28.
26 M. F. Acquavella, M. E. Evans, S. W. Farraher, C. J. Névoret and C. J. Abelt, *J. Org. Chem.*, 1994, **59**, 2894.
27 H. Eggert, J. Frederiksen, C. Morin and J. C. Norrild, *J. Org. Chem.*, 1999, **64**, 3846.
28 J. Y. Kwon, N. J. Singh, H. N. Kim, S. K. Kim, K. S. Kim and J. Yoon, *J. Am. Chem. Soc.*, 2004, **126**, 8892.
29 Y. Liu, K. Liu, Z. Wang and X. Zhang, *Chem.–Eur. J.*, 2011, **17**, 9930.
30 C. Pierlot, S. Hajjam, C. Barthélémy and J.-M. Aubry, *J. Photochem. Photobiol., B*, 1996, **36**, 31.
31 C. Pramanik and G. P. Miller, *Molecules*, 2012, **17**, 4625.

32 Y. Wakayama, R. Hayakawa, T. Chikyow, S. Machida, T. Nakayama, S. Egger, D. G. de Oteyza, H. Dosch and K. Kobayashi, *Nano Lett.*, 2008, **8**, 3273.
33 (*a*) E. Cances, B. Mennucci and J. Tomasi, *J. Chem. Phys.*, 1997, **107**, 3032; (*b*) M. Cossi, V. Barone, B. Mennucci and J. Tomasi, *Chem. Phys. Lett.*, 1998, **286**, 253; (*c*) B. Mennucci and J. Tomasi, *J. Chem. Phys.*, 1997, **106**, 5151.
34 M. J. Frisch, G. W. Trucks, H. B. Schlegel, G. E. Scuseria, M. A. Robb, J. R. Cheeseman, J. A. Montgomery Jr, T. Vreven, K. N. Kudin, J. C. Burant, J. M. Millam, S. S. Iyengar, J. Tomasi, V. Barone, B. Mennucci, M. Cossi, G. Scalmani, N. Rega, G. A. Petersson, H. Nakatsuji, M. Hada, M. Ehara, K. Toyota, R. Fukuda, J. Hasegawa, M. Ishida, T. Nakajima, Y. Honda, O. Kitao, H. Nakai, M. Klene, X. Li, J. E. Knox, H. P. Hratchian, J. B. Cross, C. Adamo, J. Jaramillo, R. Gomperts, R. E. Stratmann, O. Yazyev, A. J. Austin, R. Cammi, C. Pomelli, J. W. Ochterski, P. Y. Ayala, K. Morokuma, G. A. Voth, P. Salvador, J. J. Dannenberg, V. G. Zakrzewski, S. Dapprich, A. D. Daniels, M. C. Strain, O. Farkas, D. K. Malick, A. D. Rabuck, K. Raghavachari, J. B. Foresman, J. V. Ortiz, Q. Cui, A. G. Baboul, S. Clifford, J. Cioslowski, B. B. Stefanov, G. Liu, A. Liashenko, P. Piskorz, I. Komaromi, R. L. Martin, D. J. Fox, T. Keith, M. A. Al-Laham, C. Y. Peng, A. Nanayakkara, M. Challacombe, P. M. W. Gill, B. Johnson, W. Chen, M. W. Wong, C. Gonzalez and J. A. Pople, *Gaussian 03, Revision E.01*, Gaussian, Inc., Wallingford, CT, 2004.
35 F. B. Sayyed and C. H. Suresh, *J. Phys. Chem. A*, 2012, **116**, 5723.
36 M. Duan, B. Song, G. Shi, H. Li, G. Ji, J. Hu, X. Chen and H. Fang, *J. Am. Chem. Soc.*, 2012, **134**, 12104.
37 B. T. King, B. C. Nool and J. Michl, *Collect. Czech. Chem. Commun.*, 1999, **64**, 1001.
38 K. Hoffmann and E. Weiss, *J. Organomet. Chem.*, 1974, **67**, 221.
39 A. Kumar, S. Sista and Y. Yang, *J. Appl. Phys.*, 2009, **105**, 094512.
40 J. Yu, Y. Zang, H. Li and J. Huang, *Thin Solid Films*, 2012, **520**, 6653.
41 D. Gupta, M. Bag and K. S. Narayan, *Appl. Phys. Lett.*, 2008, **92**, 093301.